NASA

Technical Memorandum 86187

TEMPORAL AND SPECTRAL CHARACTERISTICS OF SOLAR FLARE HARD X-RAY EMISSION

B.R. Dennis, A.L. Kiplinger, Larry E. Orwig, and K.J. Frost

JANUARY 1985

National Aeronautics and
Space Administration

Goddard Space Flight Center
Greenbelt, Maryland 20771

TM 86187

TEMPORAL AND SPECTRAL CHARACTERISTICS OF SOLAR FLARE HARD X-RAY EMISSION

by
Brian R. Dennis, Alan L. Kiplinger, Larry E. Orwig, and Kenneth J. Frost

Solar Physics Branch, Code 682
Laboratory for Astronomy and Solar Physics

Presented by K.J. Frost at the Second Indo-US Workshop on Solar Terrestrial Physics, January 20 - February 3, 1984. National Physical Laboratory, New Delhi 110012, India

January 1985

NASA Goddard Space Flight Center
Greenbelt, MD 20771 U.S.A.

Abstract

We present SMM observations of three flares that impose stringent constraints on physical models of the hard X-ray production during the impulsive phase. Hard X-ray imaging observations of the flare on 1980 November 5 at 22:33 UT show two patches in the 16-30 keV HXIS images that are separated by 7×10^4 km and that brighten simultaneously to within ~ 5 s. Observations in O V from one of the footpoints show simultaneity of the brightening in this transition zone line and in the total hard X-ray flux to within a second or two. These results suggest but do not require the existence of electron beams in this flare. The rapid fluctuations of the hard X-ray flux in some flares on time scales of < 1 s also provide evidence for electron beams and limits on the time scale of the energy release mechanism. Observations of a flare on 1980 June 6 at 22:34 UT show variations in the > 28 keV X-ray counting rate from one 20 ms interval to the next over a period of 10 s. A flare on 1980 May 10 at 17:57 UT showed extremely impulsive behavior for a period of 40 s. The hard X-ray spectral variations measured with 128 ms time resolution for one 0.5 s spike during this flare are consistent with the predictions of a thick-target, non-thermal, beam model. The model assumes that all the electrons that produce the hard X-ray spike are injected simultaneously and instantaneously at the top of a coronal loop. The electrons are followed in the model as they spiral around the assumed straight and parallel magnetic field lines down to the footpoints of the loop where they produce the bulk of the X-rays in thick-target inter-

actions. The model predictions of the spike rise and fall times and the spectral softening agree with the observations for a semicircular loop with a half length of $(1\text{-}3)\times10^9$ cm. Good agreement is only obtained, however, if the initial electron distribution is deficient at pitch angles $\gtrsim 80°$.

1. Introduction

It is almost universally accepted that solar flare hard X-rays are electron-ion bremsstrahlung. Since the bremsstrahlung cross section as a function of energy is well known, it is possible to determine the energy spectrum of the emitting electrons given the measured X-ray spectrum. Unfortunately, the interpretation of this result depends on the temperature and density of the ambient plasma with which the electrons are interacting. Three basic models have been proposed for the production of the hard X-rays: thick and thin target interactions, and thermal (Brown 1971, Lin and Hudson 1976, Tucker 1975, and Crannell et al. 1978). It is necessary to know, in any particular flare, which model (or combination of models) is correct since the determination of the electron spectrum from the observed X-ray spectrum depends on the model assumed. More importantly, the correct model must be known in order to determine the role of the fast electrons in the overall flare energetics, and ultimately to determine the fundamental energy release mechanism or mechanisms of the flare.

Hard X-ray observations of the so-called footpoint flares with instrumentation on the Solar Maximum Mission (SMM) have enabled us to determine that the thick target model is most likely to be the correct one, at least during the early part of the impulsive phase of these flares and for a significant fraction of the total X-ray flux. Observations of UV lines produced at temperatures characteristic of the transition region support this conclusion. Hard X-ray and UV observa-

tions of one such footpoint flare that occurred in 1980 on November 5 are presented in this paper not only to demonstrate this conclusion but also to show that a $\gtrsim 10^8$ K thermal source may also have existed during this flare.

Another result from SMM observations concerns the rapid fluctuations of the hard X-ray flux in some flares on time scales as short as a few tens of milliseconds. Again these data can be interpreted on the basis of a thick target model, and the analysis of one particularly well observed fast spike is presented here. It is also possible, however, that a rapidly varying $> 10^8$ K thermal source could also produce the observed fluctuations.

2. The Footpoint Flares of 1980 November 5

Comprehensive observations of two homologous flares on 1980 November 5 at 22:26 UT and 22:33 UT were made with SMM instrumentation. The Hard X-Ray Imaging Spectrometer (HXIS, Van Beek et al. 1980) obtained images with 8"x8" spatial resolution and 9 s temporal resolution in six logarithmically spaced energy bands between 3.5 and 30 keV, the Hard X-Ray Burst Spectrometer (HXRBS, Orwig, Frost and Dennis 1980) obtained spatially integrated spectra in the energy range from 30 to 500 keV every 128ms, and the Ultraviolet Spectrometer and Polarimeter (UVSP, Woodgate et al. 1980) obtained images of part of the flare volume in OV at 1371Å with a spatial resolution of 10"x10" and a temporal resolution of ~ 1 s. The X-Ray Polychromator (Acton et al. 1980) also made observations of these

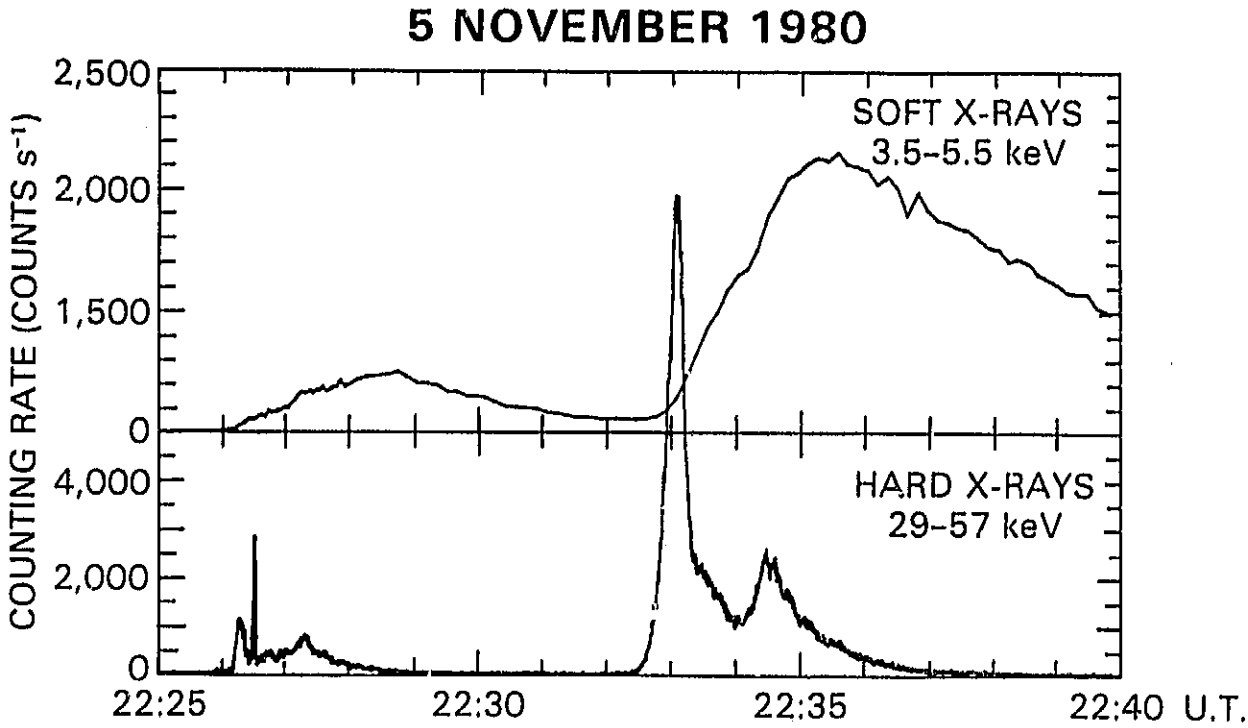

Figure 1. Soft and hard X-ray emissions as a function of time for the two flares on 1980 November 5. The soft X-ray counting rate is the sum of the counts in the HXIS band 1 in selected pixels of the coarse field of view. The hard X-ray rate is the sum of counts in HXRBS channels 1 and 2.

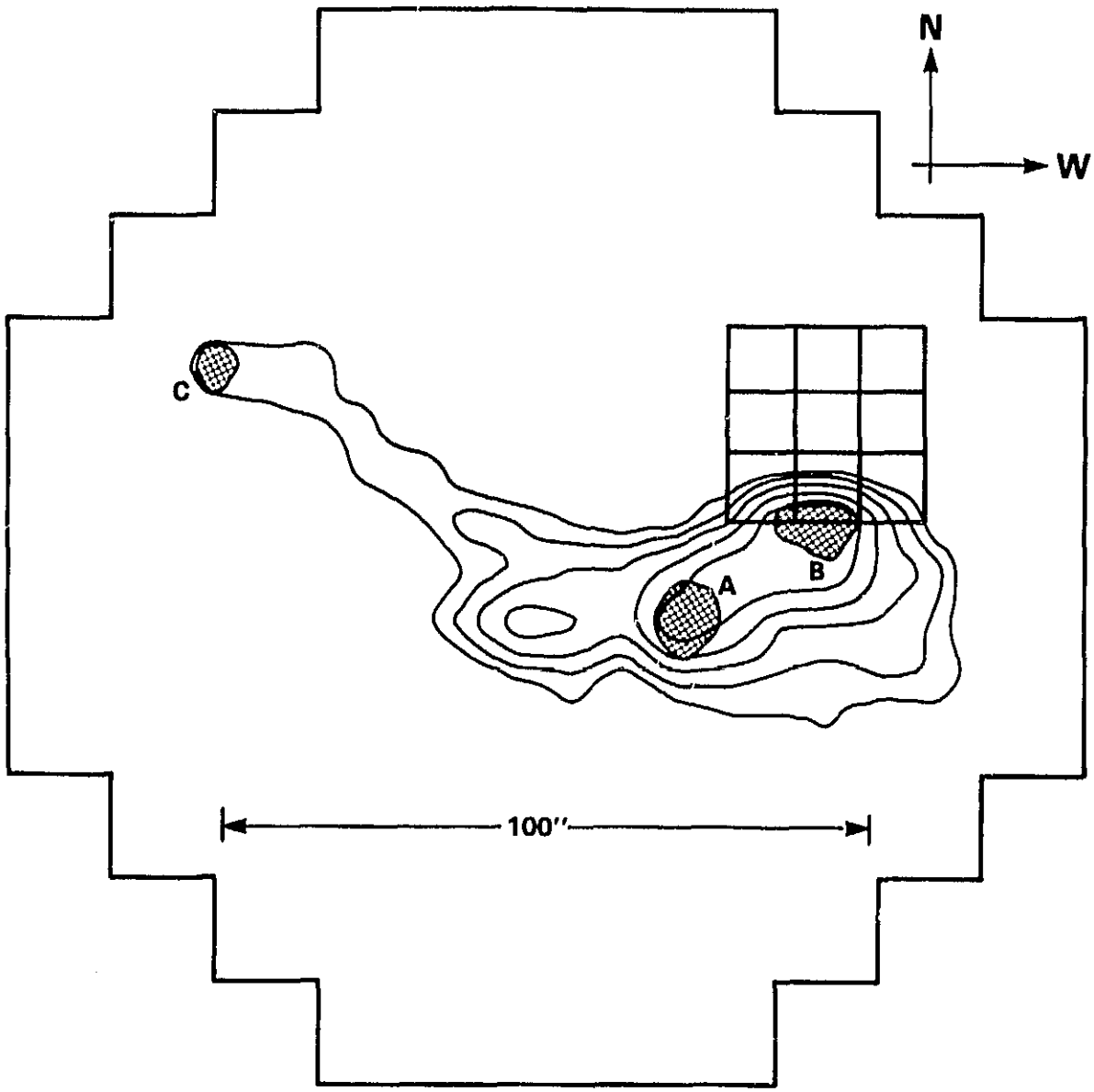

Figure 2. Contour plot obtained from the sum of three HXIS images showing the location of the soft and hard X-ray emission at the time of the most intense hard X-ray peak on 1980 November 5. Accumulation of the first image began at 22:32:53 UT. Each image had an accumulation time of 4.5 s with a 4.5 s gap between images. The contour lines were obtained from the 3.5 – 8 keV data with the collimator response deconvolved according to the method given by Svestka *et al.* (1983). The contour levels are at the following counts/pixel: 25, 50, 100, 200 and 400; the deconvolved peak rate was 902 counts/pixel. The cross-hatched areas labelled A, B and C were obtained from the 16-30 keV data similarly deconvolved. The outer edge of these areas corresponds to a contour level of 40 counts/pixel for A and B and 20 counts/pixel for C with a deconvolved peak rate at 53 counts/pixel. The 3×3 array of 10″×10″ squares represents the 9 UVSP pixels used for the OV observations shown in Figure 4.

flares (Antonucci, Gabriel, and Dennis, 1984).

The soft and hard X-ray time profiles in Figure 1 show that the two flares were temporally similar and Hα images show that they were also spatially homologous. Although the first flare was observed at 15 GHz with the Very Large Array (Hoyng et al., 1983), it was a factor of ten less intense in X-rays than the second flare and the statistical significance of the HXIS images in the highest energy bands (16-30 keV) is poor. Hence, the second flare has been the subject of more extensive study than the first flare (Duijveman, Hoyng and Machado 1982; Duijveman and Hoyng, 1983; Rust, Simnett and Smith, 1984; MacKinnon, Brown and Hayward, 1984; Wu et al. 1984). The HXIS 16-30 keV images show three well resolved bright patches during the first impulsive peak at 22:33 UT (Figure 2). Two patches labelled A and B following Duijveman, Hoyng and Machado (1982) are separated by 1.6×10^4 km and a third patch labelled C is separated from B by 7.0×10^4 km. Comparisons with Hα images and magnetograms lead Duijveman, Hoyng and Machado (1982) to conclude that the bright patches were at the footpoints of two magnetic loops joining A and B, and B and C. They further argued from the simultaneity of the peaks in the 16-30 keV counting rate at B and C that the most likely explanation for these bright patches was that electrons travelled down the legs of the loops and produced the X-rays in thick target interations at the footpoints. The simultaneity of the peaks can be judged from Figure 3 where the measured counting rates at the three footpoints are shown as a function of time together with the total rate observed with

HXRBS at a somewhat higher energy. Duijveman et al. (1982) claimed that the footpoints B and C started to brighten simultaneously to within ~ 5 s implying a velocity of $> 2 \times 10^9$ cm s^{-1} along the assumed semicircular loop. They showed that for this velocity to be interpreted as an Alfven velocity, the magnetic field in the loop must have been $\gtrsim$ 900 G, implausibly high for such a large loop. They concluded that the most likely explanation for the simultaneous brighting was a beam of fast electrons.

The bulk of the flare energy is concentrated in and around A and B, however, and the simultaneity argument cannot rule out MHD disturbances or thermal conduction as plausible energy transport mechanisms over the shorter distances involved in the loop, or loops, joining these two points. UVSP observations covering the 3x3 array of 10"x10" pixels shown in Figure 2 at and near footpoint B have much better time resolution and show excellent correlation with the total hard X-ray emission. This is shown in Figure 4 where the time variation of the OV counting rate from all 9 UVSP pixels summed together is plotted for comparison with the HXRBS counting rate. In this case simultaneity is established to a few seconds. This is still not sufficient to prove the existence of an electron beam in loop AB, but in other flares where UV - hard X-ray simultaneity has been established to ~ 1s, an expanding thermal source at the top of a loop has been shown to be inconsistent with the observations (Woodgate et al. 1983). The spikes in the OV rate in the pixels furthest from footpoint B are only ~ 1% of the highest intensity in the other pixels (see Figure 5) and consequently are believed to result from leakage

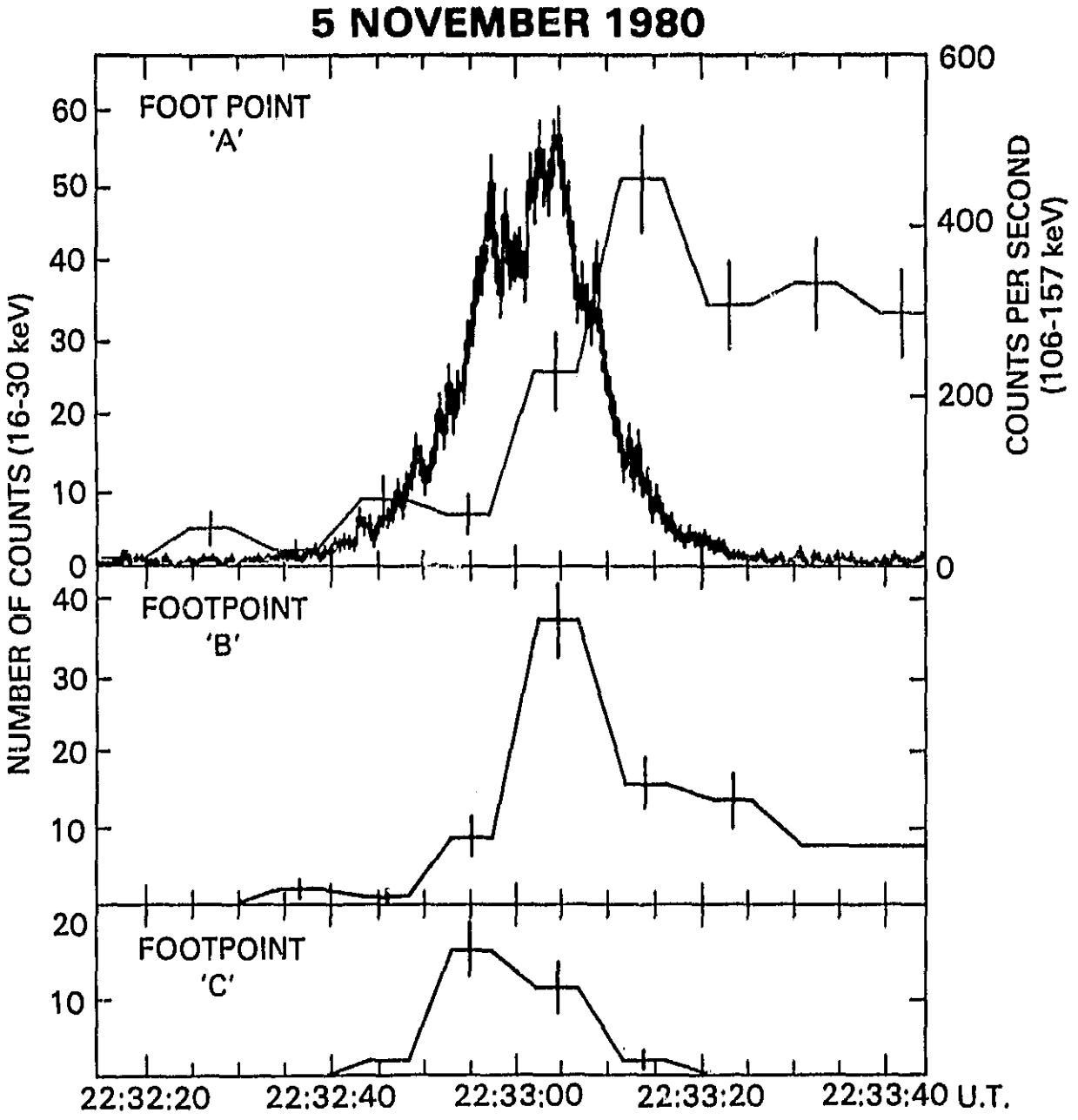

Figure 3. Time variations of the HXIS counting rate in the 16-30 keV energy range from footpoints A (pixels 329 and 349), B (385 and 389) and C (166 and 180) indicated in Figure 2 together with the HXRBS counting rate in the 106 to 157 keV range. The vertical error bars for both the HXIS and HXRBS data represent $\pm$ 1σ statistical uncertainties, and the horizontal lines through the HXIS data points represent the 4.5 s accumulation time per image with 4.5 s gaps between observations. The HXRBS integration time was 0.128 s per point.

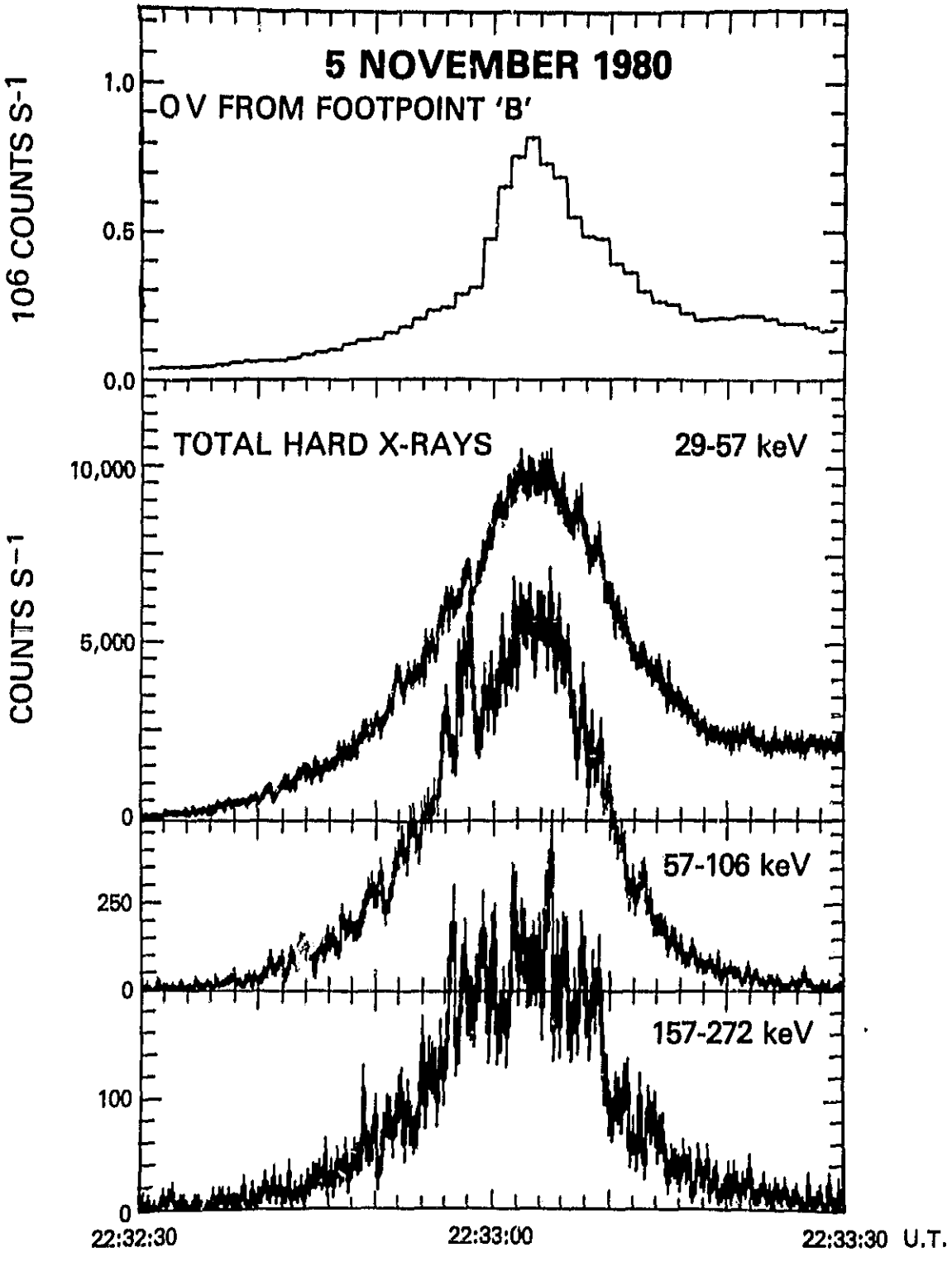

Figure 4. Time variation of the UVSP counting rate in OV summed over all 9 pixels shown in Figure 2 together with the HXRBS counting rates in three energy bands.

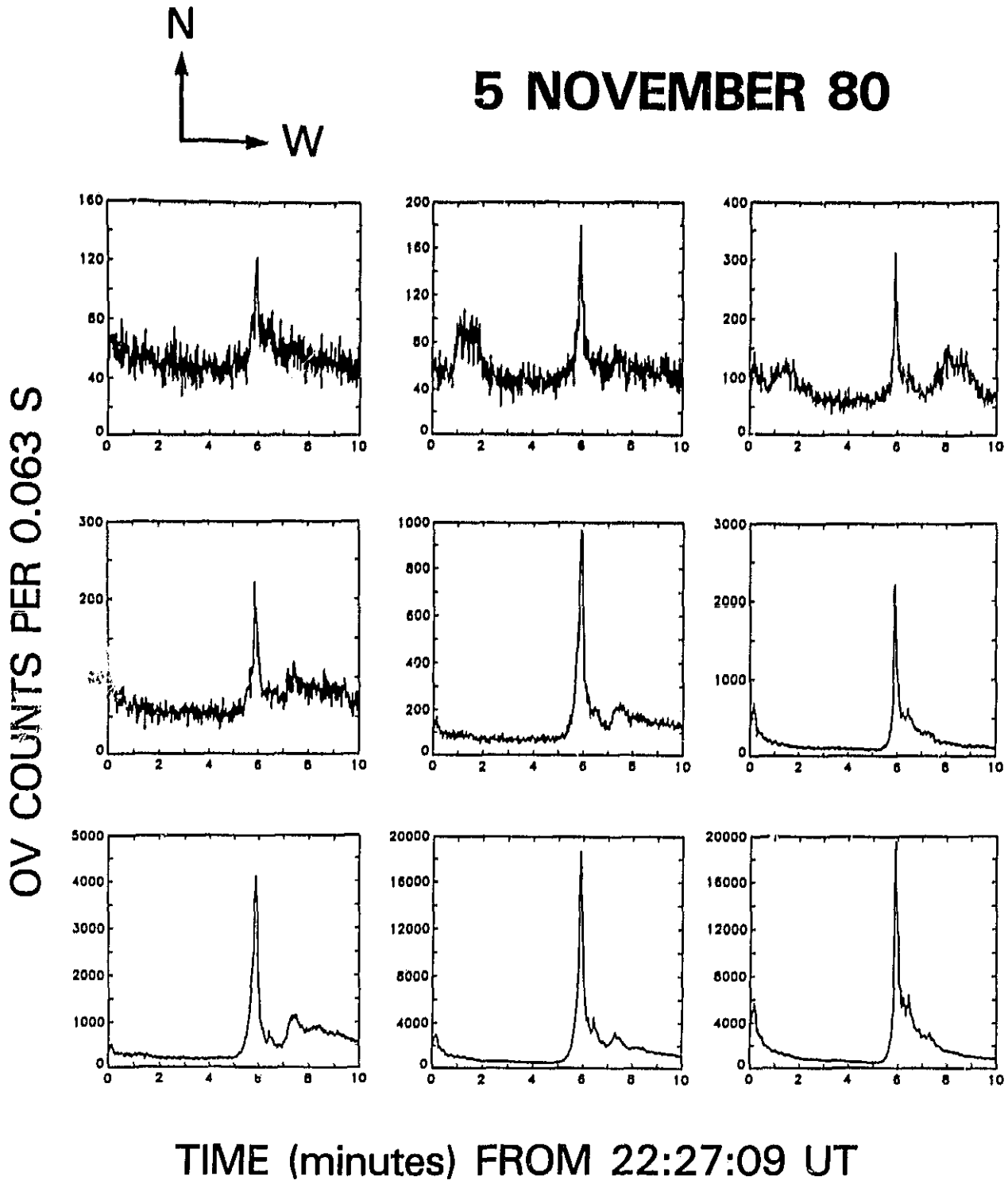

Figure 5. Light curves of the UVSP counting rates in OV for the nine individual pixels arranged as they appear in Figure 2. Note that the vertical scale is different for each pixel. One 63 ms observation was made in each pixel every 1.216 s.

between pixels (Woodgate, private communication).

MacKinnon, Brown and Hayward (1984) have shown that only a small fraction of the hard X-rays in the HXIS 16-30 keV images come from the pixels that define the bright patches A, B, and C. They claim that the remainder come from a diffuse region around A and B although the interpretation of the 2 or 3 images at the time of the first hard X-ray burst is complicated by the presence of a diffuse background resulting from the leakage of high energy photons through the walls of the instrument collimator. The conclusion that only a small fraction of the photons come from the footpoints is supported, however, by an extrapolation of the HXRBS spectrum above 30 keV down to the 16-30 keV HXIS energy range. Good agreement is found with the total HXIS counting rate integrated over the coarse field of view. When the counts in only the fine field of view pixels that define the three bright patches are summed, however, the resulting flux is a order of magnitude below the HXRBS extrapolation. If the spectrum of only the impulsive component is used, i.e. the more gradually varying component is subtracted from the fluxes in each energy band, then the spectrum becomes flatter at energies below 50 keV, E^{-3} compared to $E^{-3.9}$ for the spectrum of the total flux. This reduces the discrepancy and suggests that the impulsive component comes primarily from the footpoints whereas the more gradually varying component comes from a larger area.

Rust (1984) has also suggested that the total energy in the beams in the November 5 flare was $\leq$ 10% of the total energy released and that

the remainder appeared as a high temperature thermal source. Evidence from HXIS images in bands 1 and 2 for a thermal conduction front travelling to point C is given in
Rust, Simnett and Smith (1984) but the interpretaion of the moving contour lines is ambiguous. An equally valid interpretation would be one where the emission from loop BC increased uniformly along the loop as the plasma in the loop was heated by fast electrons travelling along the loop.

Later on in the same flare at 22:34:30 UT, a second hard X-ray peak occurred but with a much softer spectrum, E^{-7} or steeper compared to E^{-4} at the time of the first peak. Furthermore, at the time of the second peak, the HXIS images show that the 16-30 keV X-rays came predominantly from a location between the original bright patches A and B. The soft X-ray flux shows a second step increase at about this time, as indicated in Figure 1, suggesting that almost the same amount of energy was released as during the first impulsive peak. The simplest explanation of these observations is that this second energy release served mainly to heat the plasma injected into the loop as a result of the first non-thermal energy release. Such a transition from an essentially non-thermal model to a thermal model during the impulsive phase of many flares has been proposed by Smith (1984) and is interpreted in his dissipative thermal model, a term originally suggested by Emslie and Vlahos (1980). Smith (1984) suggests that an increase in the ratio of plasma to magnetic pressure (the plasma β) at the energy release site later in the flare results in this transition from a non-thermal to a thermal model. It

must be pointed out, however, that the blue shifts in the Ca XIX lines observed with the Bent Crystal Spectrometer (Acton et al. 1980) persist into the later stages of the impulsive phase of the 1980 November 5 flare indicating continuing chromospheric evaporation with upward velocities of ~ 200 km s^{-1} even during the second hard X-ray peak (Antonucci, Gabriel and Dennis, 1984).

It is clear that given the available photon counting statistics, and the spatial and temporal resolution of the observations of the 1980 November 5 flare, an unambiguous interpretation of the results is not possible. Nevertheless, it still appears that beams of fast electrons must have existed during the flare, at least during the first impulsive hard X-ray peak. They may have constituted only 10% of the total flare energy but that still amounts to 2×10^{29} ergs (Wu et al. 1984).

3. Rapid Fluctuations of Hard X-Ray Fluxes with Constraints on Models

We now have clear evidence of very rapid variations in hard X-rays with timescales of less than 1 s (Hurley and Duprat 1977; Kiplinger et al. 1983a; Hurley et al. 1983). Observations with HXRBS since the launch of SMM in 1980 have revealed hundreds of examples of fast spikes with durations of less than 1 s. An excellent example of rapid fluctuations is provided by a flare on 1980 June 6 at 22:34 UT, 3.5 h before the well known gamma ray line event of 1980 June 7 (cf. Kiplinger et al. 1983b). Both events occurred in active region 2495. Two seconds of HXRBS (28-484 keV) memory data of the June 6 event are plotted in Figure 6 at a time

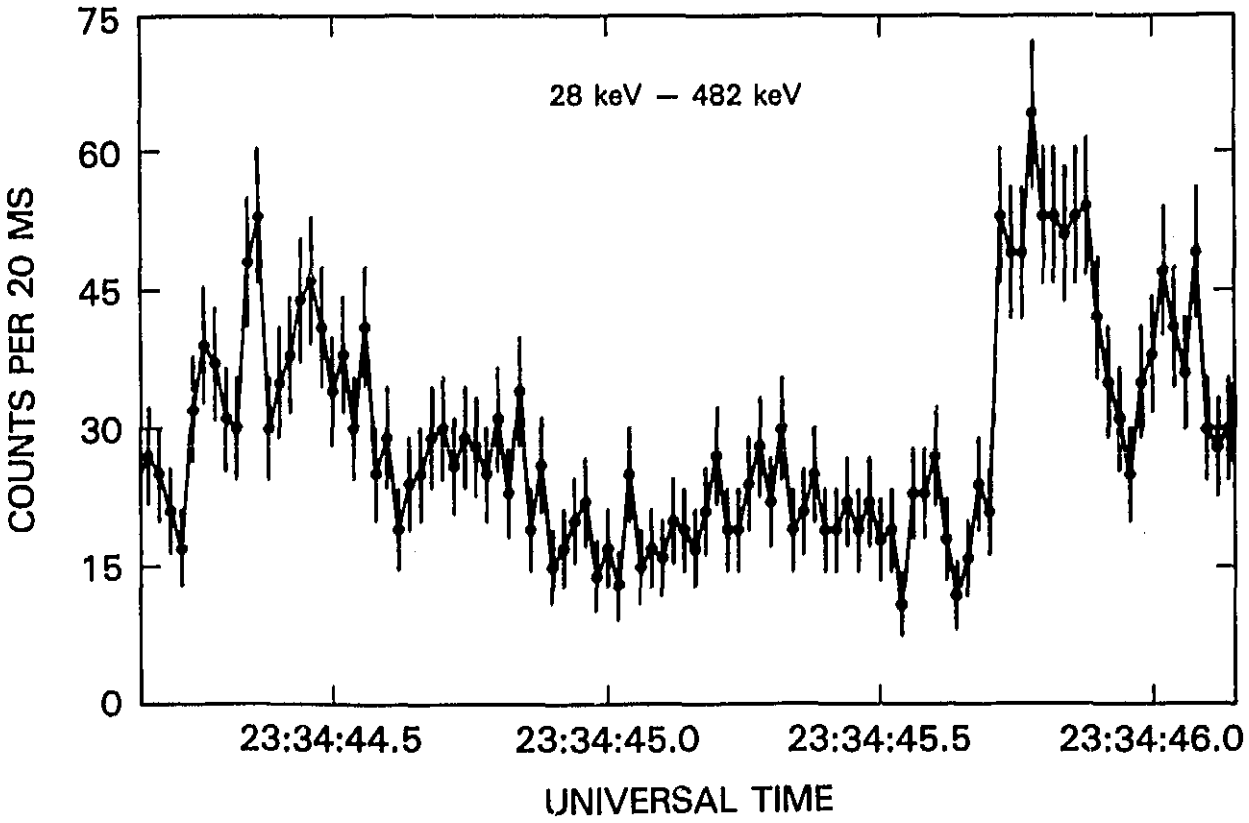

Figure 6. Two seconds of HXRBS memory data showing very rapid hard X-ray variations in a solar flare which occurred on 1980 June 6. The counting rate is plotted at a time resolution of 20 ms per point with $\pm$ 1σ statistical error bars.

resolution of 20 ms. The most dramatic variation is the large, unresolved rise from 21 to 53 counts per 20 ms at 23:34:45.7 UT. The realization of a value of 53 from a Poisson distribution with a mean of 21 has a probability of $\sim 2 \times 10^{-9}$. Since there are only $\sim 3 \times 10^{4}$ 20 ms intervals with counts of 21 or higher in the surveyed data, one would not expect such a transition by chance. Numerous other fast variations (not shown) occurring within 10 s of the plotted interval also support the reality of the rapid fluctuations shown in Figure 6.

Clearly, such variations impose constraints for physical models of hard X-ray production (see for example Kiplinger et al. 1983a) that need to be explored. Recently Emslie (1983) has developed a thick-target non-thermal beam model that is capable of predicting the time-dependent hard X-ray behavior resulting from an instantaneous injection of electrons into the top of a coronal loop. We have further developed this model in order to provide quantitative, time-dependent hard X-ray fluxes computed over the HXRBS energy range (Kiplinger, et al. 1984).

A prime example of a flare exhibiting fast variations that are suitable for comparison with the model predictions occurred on 1980 May 10 in NOAA active region 2438 (S14E29). The event was classified as C4 in soft X-rays and as SN in optical importance. Patrol photographs from Sacramento Peak Observatory show a compact flare approximately 1.4×10^{4} km across that directly preceeds the leader spot of the active region. Although the photographs of the flare show little or no structure in Hα, they do reveal a considerable amount of surge activity both during and

after the event. The extremely impulsive behavior of this flare is shown in the 40 s section of the HXRBS time profile plotted in Figure 7a with a time resolution of 128 ms. An 8 s subinterval is replotted on an expanded time scale in Fig. 7b with ± 1σ statistical error bars. The intense fast spike at 17:57:46 UT is of particular interest since it shows rise and decay times (defined here as the time to change from 0 - 100% in intensity and vice versa) of 0.25 s and 0.4 s, respectively.

In modeling the event, we adopted Emslie's time dependent non-thermal model which was developed to interpret short time scale hard X-ray bursts (Emslie 1983). The present model assumes that electrons are injected instantaneously at the top of a coronal loop of half length L with a differential power-law spectrum in electron energy E of the form $f(E) \propto E^{-\delta}$ electrons keV^{-1}. The electrons also are assumed to have a uniform pitch angle distribution over the range of pitch angles from θ_1 to θ_2 and the guiding magnetic field lines are assumed to be straight and parallel. Hence, the magnetic field does not cause mirroring of the electrons. Although the model accounts for Coulomb collisions and bremsstrahlung occurring within the loop, such effects are unimportant for the models computed here. The present version of the model has been modified to include the total number of electrons with energies above 25 keV, $N_{>25}$, as a variable parameter. Knowledge of the total number of electrons immediately allows one to compute their total energy, $W_{>25}$; moreover, it permits the computation of absolute X-ray fluxes, which may be directly compared with observations.

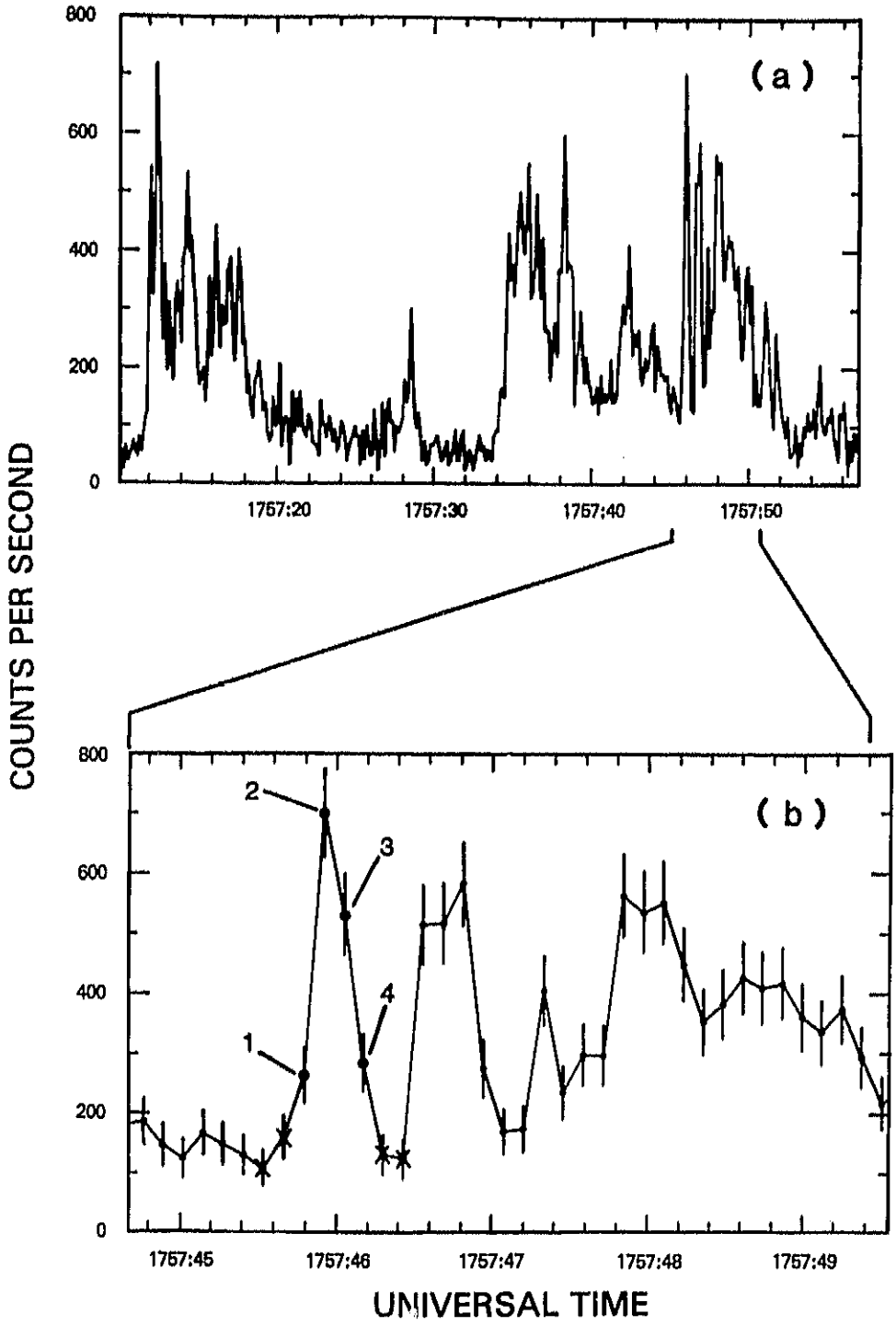

Figure 7. Hard X-ray time profiles (27-496 keV) of a solar flare which occurred on 1980 May 10. The curve in (a) shows 40 s of the most impulsive phase of the event at a time resolution of 128 ms. The curve in (b) is an expanded version of the region connected by lines to (a) with $\pm$ 1σ statistical error bars drawn vertically through each point. Crosses in (b) show the points that were used for background subtraction in the determination of spectra at the four numbered times on the spike.

Models corresponding to the X-ray peak at 17:57:46 UT were constructed with various loop half-lengths, L. Since a semi-circular loop whose footpoints span the observed Hα region as described above would have $L \simeq 1.4 \times 10^4$ km, models corresponding to this scale were examined first. The observed and the best fitting theoretical spectra obtained during the spike are shown in Figures 8a - 8d. Clearly the model fits the observations well. Values of various parameters of the model (model 1) used to produce the theoretical spectra shown in Fig. 8 are given in Table 1. Equally good agreement is also found between the predicted and observed X-ray spectra for calculations with larger L such as model 2 of Table 1. Predicted X-ray spectra have been computed for models with L as small as 10^8 cm, but the parameters cannot be adjusted to give satisfactory agreement with the measured spectra for loops this small. Note that a nearly, but not quite, isotropic electron distribution is needed to obtain the good agreement. Models with larger values of L require the initial electron distribution to be more highly beamed down the field lines of the loop in order to maintain the observed decay time. This suggests that electrons with pitch angles $\theta \gtrsim 78°$ either are not produced or they are mirrored before they reach the chromosphere.

A pleasing result of the modeling is that analysis of the hard X-ray spectra alone leads one to an acceptable range in the quantative dimensions of the loop. Another satisfying aspect of the analysis is that the progressive softening of the measured hard X-ray spectra during the decline is echoed by the computed spectra although this softening cannot

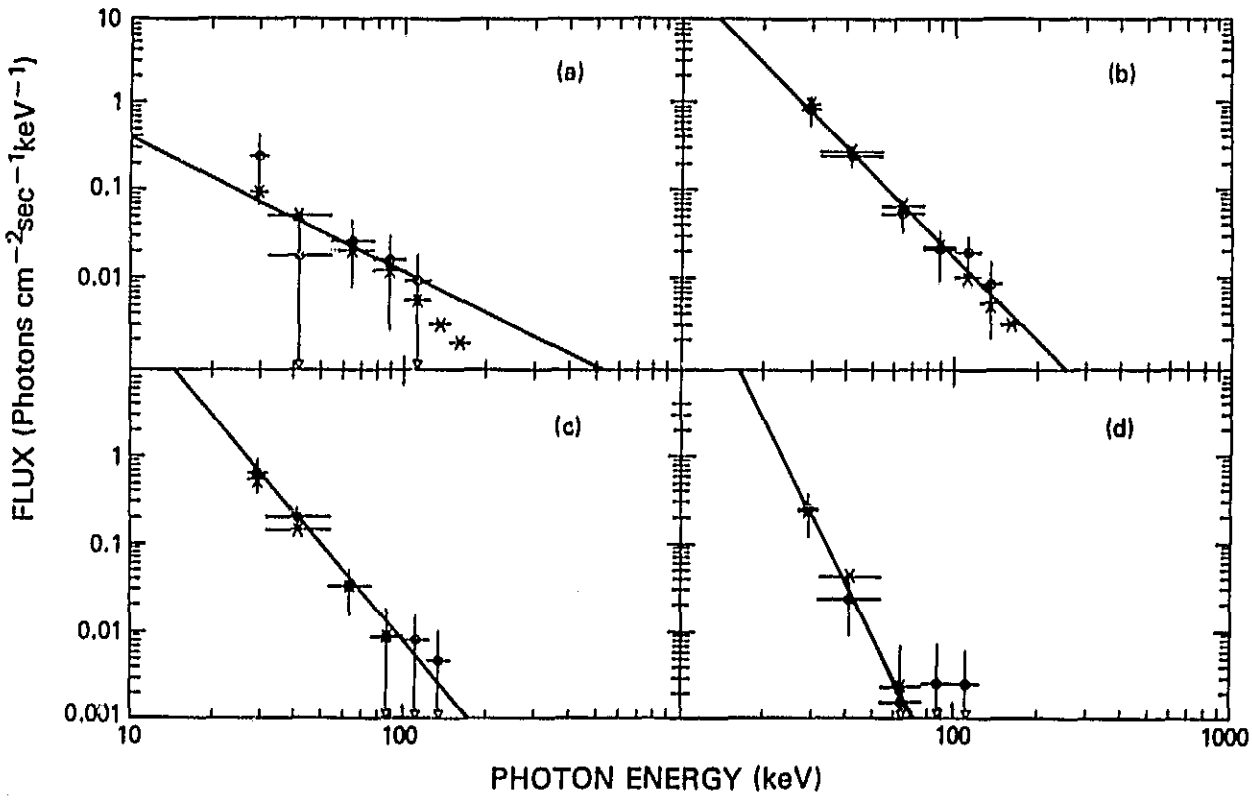

Figure 8. Observed spectra (open circles) and theoretical spectra (crosses) on the rise (a), at the peak (b), and on the decline (c and d) of the X-ray spike obtained at the time of the points numbered 1 to 4, respectively, in Figure 7(b). Horizontal bars represent HXRBS channel widths while the vertical bars on the observed points reflect $\pm$ 1σ statistical uncertainties.

TABLE 1.

Parameters of Non-Thermal Models

Parameters*	Model 1	Model 2
L	1.4×10^9 cm	3.0×10^9 cm
δ	4.5	5.0
$N_{>25}$	1.3×10^{34}	1.8×10^{34}
θ_1	78°	60°
θ_2	0°	0°
n_c	3.0×10^{10} cm^{-3}	3.0×10^{10} cm^{-3}
$W_{>25}$	7.8×10^{26} ergs	9.6×10^{26} ergs

*All parameters are described in the text except for the following: the coronal density, n_c, is an input parameter which has little effect on electron propagation for the models considered here; $W_{>25}$, the total energy in the electrons above 25 keV, is a derived parameter.

be controlled through adjustments of the model parameters.

4. Summary and Conclusions

We have decribed observations of a footpoint flare and an extremely impulsive flare both of which show evidence for the existence of electron beams and the production of hard X-rays in thick-target interactions. In the footpoint flare the electron beams contained $> 2 \times 10^{29}$ ergs and lasted for ~ 30 s. In the impulsive flare, the hard X-ray spectral evolution is fully consistent with the instantaneous injection of electrons into the top of a coronal loop with half length of $5 \times 10^{8} < L < 5 \times 10^{9}$ cm and the subsequent X-ray emission as the electrons are beamed to the footpoints. In view of the fact that there is evidence in HXRBS data for X-ray rise and decay times as short as 20 ms and spikes with full widths at half maximum as short as 45 ms, very short electron injection times may indeed be present in some events.

From global theoretical arguments invoking Faraday's Law, Spicer (1983) and Holman (1984) argue that flare mechanisms that accelerate electrons by means of dissipating pre-flare magnetic energy stored insitu cannot produce electron fluxes large enough to explain the bulk of the hard X-rays observed in flares as non-thermal bremsstrahlung. The magnitudes of the beam currents required to explain the observations of the flares discussed in this paper are such that their arguments apply. However, this should not be interpreted as ruling out a non-thermal hypothesis for these events. Spicer (1983) points out that models that

generate a co-spatial beam return current can satisfy the non-thermal hypothesis. One mechanism which can produce such a return current is a flow field (eg. a shock front) moving across a magnetic field and is referred to as a "capacitive" flare mechanism by Spicer. The intense Hα surge activity which occurred during the impulsive X-ray phase of the 1980 May 10 flare is in accord with this concept. On the other hand, the success of the present non-thermal model does not undermine nor discredit other models, such as dissipative thermal models (cf. Brown, Melrose, and Spicer 1979; Smith and Lilliequist 1979; Smith and Auer 1980; Smith 1984), which may be capable of modeling fast hard X-ray spikes equally well. Clearly, further detailed modeling is needed.

Acknowledgements

We are grateful to members of the other SMM instrument teams for access to their data and useful discussions of the scientific implications. In particular, we thank Dick Shine for the production of the UVSP time profiles and Mike Acierno for assistance in displaying and analysing the HXIS images. We also gratefully acknowledge Gordon Emslie, who kindly provided his original code that forms the nucleus of the code employed to analyse the 1980 May 10 flare.

References

Acton, L.W. et al. 1980, Solar Phys., 65, 53.

Antonucci, E., Gabriel, A.H., and Dennis, B.R. 1984, Ap.J., in press.

Brown, J.C. 1971, Solar Phys, 18, 489.

Brown, J.C., Melrose, D.B., and Spicer, D.S. 1979, Ap. J., 228, 592.

Crannell, C.J., Frost, K.J., Matzler, C., Ohki, K., and Saba, J. 1978, Ap.J., 223, 620.

Duijveman, A., Hoyng, P., and Machado, M.E. 1982, Solar Phys., 81, 137.

Duijveman, A., and Hoyng, P. 1983, Solar Phys., 86, 289.

Emslie, A.G. and Vlahos, L. 1980, Ap.J., 242, 359.

Emslie, A.G. 1983, Ap.J., 271, 367.

Holman, G.D. 1984, NASA TM 86112, submitted to Ap.J.

Hoyng, P., Marsh, K.A., Zirin, H., and Dennis, B.R. 1983, Ap.J., 268, 865.

Hurley, K. and Duprat, G. 1977, Solar Phys., 52, 107.

Hurley, K., Niel, M., Talon, R., Estulin, I.V. and V.Ch. Dolidze 1983, Solar Phys., 86, 367.

Kiplinger, A.L., Dennis, B.R., Emslie, A. G., Frost, K.J. and Orwig, L.E., 1983a, Ap.J. Lett., 265, L99.

Kiplinger, A.L., Dennis, B.R., Frost, K.J. and Orwig, L.E.,1983b, Ap.J., 273, 783.

Kiplinger, A.L., Dennis, B.R., Frost, K.J. and Orwig, L.E. 1984, Ap.J. Lett., in press.

Lin, R.P. and Hudson, H.S. 1976, Solar Phys., 50, 153.

Orwig, L.E., Frost, K.J., and Dennis, B.R. 1980, Solar Phys. 65, 25.

MacKinnon, A.L., Brown, J.C., and Hayward, J., 1984, preprint.

Rust, D.M., Simnett, G.M., and Smith, D.F. 1984, Ap.J., submitted.

Rust, D.M. 1984, Advances in Space Research, Proc. 25th Plenary Meeting of COSPAR, Graz, Austria (Pergamon Press, Oxford).

Smith, D.F. and Lilliequist, C.G. 1979 Ap. J., 232, 582.

Smith, D.F. and Auer, L.H. 1980, Ap. J., 238, 1126.

Smith, D.F. 1984, Ap.J., in press.

Spicer, D.S. 1983, Adv. Space Res., 2, 135.

Svestka, Z. et al. 1983, Solar Phys., 85, 313.

Tucker, W.H. 1975, Radiation Processes in Astrophysics (Cambridge: MIT Press).

Van Beek, H.F., Hoyng, P., Lafleur, B., and Simnett, G.M. 1980, Solar Phys., 65, 39.

Woodgate, B.E. et al. 1980, Solar Phys., 65, 73.

Woodgate, B.E., Shine, R.A., Poland A.I., and Orwig, L.E. 1983, Ap.J., 265, 530.

Wu, S.T. et al. 1984, Proc. SMM Workshop on Solar Flares (B.E. Woodgate and M.R. Kundu, eds.), in preparation, ch. 4.